Received: 3 December 2021 | Revised: 30 April 2022 | Accepted: 11 May 2022

DOI: 10.1096/fj.202101812R

THE FASEB JOURNAL

RESEARCH ARTICLE

Dissecting the relationship between plasma and tissue metabolome in a cohort of women with obesity: Analysis of subcutaneous and visceral adipose, muscle, and liver

Zhanxuan E. Wu[1,2,3] | **Marlena C. Kruger**[2,4] | **Garth J. S. Cooper**[5,6,7] | **Ivana R. Sequeira**[3,5,8] | **Anne-Thea McGill**[8] | **Sally D. Poppitt**[3,4,6,8] | **Karl Fraser**[1,3,4]

[1]Food Chemistry and Structure, AgResearch Limited, Palmerston North, New Zealand

[2]School of Health Sciences, Massey University, Palmerston North, New Zealand

[3]High-Value Nutrition National Science Challenge, Auckland, New Zealand

[4]Riddet Institute, Massey University, Palmerston North, New Zealand

[5]School of Biological Sciences, University of Auckland, Auckland, New Zealand

[6]Department of Medicine, University of Auckland, Auckland, New Zealand

[7]Centre for Advanced Discovery and Experimental Therapeutics, School of Medical Sciences, University of Manchester, Manchester, UK

[8]Human Nutrition Unit, School of Biological Sciences, University of Auckland, Auckland, New Zealand

Correspondence
Zhanxuan E. Wu and Karl Fraser, Food Chemistry and Structure, AgResearch Limited, Palmerston North, 4442, New Zealand.
Email: Emily.Wu@agresearch.co.nz and karl.fraser@agresearch.co.nz

Present address
Anne-Thea McGill, School of Health & Human Sciences, Southern Cross University, Lismore, New South Wales, Australia

Funding information
Ministry for Business Innovation and Employment (MBIE), Grant/Award Number: 3710040; Manatu Hauora | Health Research Council of New Zealand (HRC), Grant/Award Number: 08/190C

Abstract

Untargeted metabolomics of blood samples has become widely applied to study metabolic alterations underpinning disease and to identify biomarkers. However, understanding the relevance of a blood metabolite marker can be challenging if it is unknown whether it reflects the concentration in relevant tissues. To explore this field, metabolomic and lipidomic profiles of plasma, four sites of adipose tissues (ATs) from peripheral or central depot, two sites of muscle tissue, and liver tissue from a group of nondiabetic women with obesity who were scheduled to undergo bariatric surgery ($n = 21$) or other upper GI surgery ($n = 5$), were measured by liquid chromatography coupled with mass spectrometry. Relationships between plasma and tissue profiles were examined using Pearson correlation analysis subject to Benjamini–Hochberg correction. Plasma metabolites and lipids showed the highest number of significantly positive correlations with their corresponding concentrations in liver tissue, including lipid species of ceramide,

Abbreviations: AA, amino acid; AT, adipose tissue; BCAA, branched-chain amino acid; BH, Benjamini–Hochberg; BMI, body mass index; CER, ceramide; DG, diacylglycerol; DSAA, deep subcutaneous abdominal adipose tissue; EICs, extracted ion chromatograms; ESI, electrospray ionization; FFA, free fatty acid; GI, gastrointestinal; GluCer, glucosylceramide; HILIC, hydrophilic chromatograph; HMDB, human metabolome database; IAA, intra-abdominal adipose tissue; IR, insulin resistance; LC-MS, liquid chromatography-mass spectrometry; LCPUFA, long-chain polyunsaturated fatty acid; LED, low energy diet; LPE, lysophosphatidylethanolamine; PC, phosphatidylcholine; PCA, principal component analysis; PE, phosphatidylethanolamine; PE-NMe2, dimethylphosphatidylethanolamine; PUFA, polyunsaturated fatty acid; QC, quality control; RAM, rectus abdominis muscle; SAA, subcutaneous abdominal adipose tissue; SM, sphingomyelin; STA, subcutaneous thigh adipose tissue; T2D, type 2 diabetes; TG, triacylglycerol; TMAO, trimethylamine oxide; VLCFA, very long acyl chain fatty acid; VLM, vastus lateralis muscle.

mono- and di-hexosylceramide, sphingomyelin, phosphatidylcholine (PC), phosphatidylethanolamine (PE), lysophosphatidylethanolamine, dimethyl phosphatidylethanolamine, ether-linked PC, ether-linked PE, free fatty acid, cholesteryl ester, diacylglycerol and triacylglycerol, and polar metabolites linked to several metabolic functions and gut microbial metabolism. Plasma also showed significantly positive correlations with muscle for several phospholipid species and polar metabolites linked to metabolic functions and gut microbial metabolism, and with AT for several triacylglycerol species. In conclusion, plasma metabolomic and lipidomic profiles were reflective more of the liver profile than any of the muscle or AT sites examined in the present study. Our findings highlighted the importance of taking into consideration the metabolomic relationship of various tissues with plasma when postulating plasma metabolites marker to underlying mechanisms occurring in a specific tissue.

KEYWORDS

biomarkers, clinical metabolomics, liquid chromatography–mass spectrometry, tissue metabolomics

1 | INTRODUCTION

Untargeted metabolomics involves the comprehensive measurement of metabolites in a biological sample and has become an emerging tool for biomarker discovery and the understanding of metabolic alterations associated with diseases.[1] Among various human sample types, plasma and serum are the blood compartments which are convenient and minimally invasive to obtain and therefore widely used for clinical chemistry diagnoses and risk screening.[2] Blood samples contain a broad range of metabolites. The Human Metabolome Project has identified and quantified over 4200 metabolites in human serum.[3] The lipid composition in human plasma also contains remarkable diversity, with more than 500 lipid species quantified.[4] Given the rich complexity of metabolites can be measured in blood, correlating the circulating metabolomic profile with phenotype or clinical outcomes can be highly informative and descriptive of many health issues. This has made the circulating metabolites important targets in clinical studies. To date, metabolomics has been successfully applied to identify circulating markers that have the potential to diagnose cardiometabolic diseases at an early stage or provide additional prognostic value.[5–8] Metabolomic profiling of blood samples has also provided a systemic snapshot of metabolic alterations under pathophysiological conditions, hence opening a window for mechanistic investigation of the underpinning pathways during disease development.[9] Despite so, a major limitation of studying the blood metabolome is that it may provide little insight into tissue site-specific abnormalities, which are usually more biologically relevant to disease pathogenesis.[10]

Tissues, on the other hand, are regions where diverse metabolic reactions take place. However, samples are more difficult to obtain for clinical studies due to the invasiveness of tissue collection procedures. Given the heterogeneity of tissue types,[11,12] and the fact that blood represents a dynamic extracellular pool for tissues/organs, a current gap in the clinical-metabolomic research field is the absence of data identifying whether specific sets of plasma metabolites reflect the concentration of their counterparts in a particular tissue. Whether a circulating candidate marker can be used as a proxy for an abnormal concentration of a corresponding tissue metabolite remains to be elucidated.

Only a few studies have investigated the relationship between concentrations of circulating metabolites and their counterparts in different tissue types, and these studies were conducted using targeted analyses, such as the profiling of free fatty acids (FFAs), acylcarnitines, and steroid hormones.[13–16] Data on other metabolites frequently reported to be associated with cardiometabolic diseases, such as ceramides, sphingomyelins (SMs), phospholipids and ether-linked phospholipids, branched-chain amino acids (BCAAs), and aromatic AAs, are lacking.[17–19] To the best of our knowledge, no study employing an untargeted metabolomics approach to gain a wide picture of the relationship between the metabolomic profile of human plasma and a range of tissue types has yet been conducted. Therefore, the primary goal of the present study is to provide data to fill this gap. Furthermore, sites of tissue types

are also important. Adipose tissue within different body depots plays different roles in disease pathogenesis, contributing differently to cardiometabolic risk,[20] and exhibiting different profiles and metabolic activity.[11,21,22] With such a high level of complexity, it is unknown whether there are inter-depot differences in the metabolomic relationship between plasma and various regional adipose depots (lower body subcutaneous, upper body subcutaneous, and intra-abdominal[23]). Likewise, different muscle tissue sites exhibit different functions and levels of activity. It is also of interest whether muscle tissue of different regions and functions (locomotor skeletal muscle vs. postural abdominal muscle) display different metabolomic relationships with plasma.

To address these gaps, a detailed investigation of the relationship between plasma and multiple AT and muscle sites in addition to liver metabolites, measured by two complementary liquid chromatography-mass spectrometry (LC-MS) platforms in an untargeted manner, was carried out. The aim of our present study was to enhance the interpretation and accelerate the translation of plasma candidate markers identified by a metabolomics approach into useful clinical screening tools.

2 | METHODS

2.1 | Study participants and samples

Women with obesity, but not type 2 diabetes (T2D), were recruited from patients scheduled for laparoscopic bariatric (weight loss) surgery, mostly sleeve gastrectomy but some Roux-on-Y bypass ($n = 21$, mean body mass index, BMI = 40.9 kg/m^2) or general upper gastrointestinal (GI) surgery ($n = 5$, mean BMI = 38.6 kg/m^2). All participants were free of diagnosed cardiovascular or other metabolic disease and underwent surgery after an overnight fast. None of the participants showed evidence for the presence of liver disease based on liver function test (Table S1). Participants undergoing bariatric surgery completed a 14-day low energy diet (LED, 4 MJ/day intake) in order to achieve ≥10% body weight loss prior to the surgery and hence immediately prior to the collection of blood and tissue samples. During the surgical procedure, blood samples, biopsies of four AT depots considered to be either "safe" peripheral (subcutaneous thigh adipose tissue, STA) or "risky" central (subcutaneous abdominal adipose tissue, SAA; deep subcutaneous abdominal adipose tissue, DSAA; intra-abdominal adipose tissue, IAA), two sites of muscle tissue (vastus lateralis muscle, VLM; rectus abdominis muscle, RAM) and liver (wedge of the right lobe) were collected (Figure 1).

Participants were recruited at Auckland City Hospital, Auckland, New Zealand. Informed written consent was obtained at the Greenlane Clinical Centre or the University of Auckland Human Nutrition Unit (trial registration-ACTRN12611000525987; ethics approval-NTX/08/10/103).

2.2 | Materials

All organic solvents for metabolite extraction, reconstitution, and LC–MS analysis (chloroform, methanol, acetonitrile, isopropanol, and formic acid) were obtained from Thermo Fisher Scientific (Auckland, New Zealand) and were of LC–MS grade except chloroform, which was of analytical grade. Milli-Q® ultrapure water was obtained from Merck Millipore (Bedford, MA, USA). Ammonium formate (Fluka™, HPLC grade) was obtained from Sigma-Aldrich (Auckland, New Zealand). Lipid internal standard 1-palmitoyl(D_{31})-2-oleoyl-sn-glycero-3-phosp

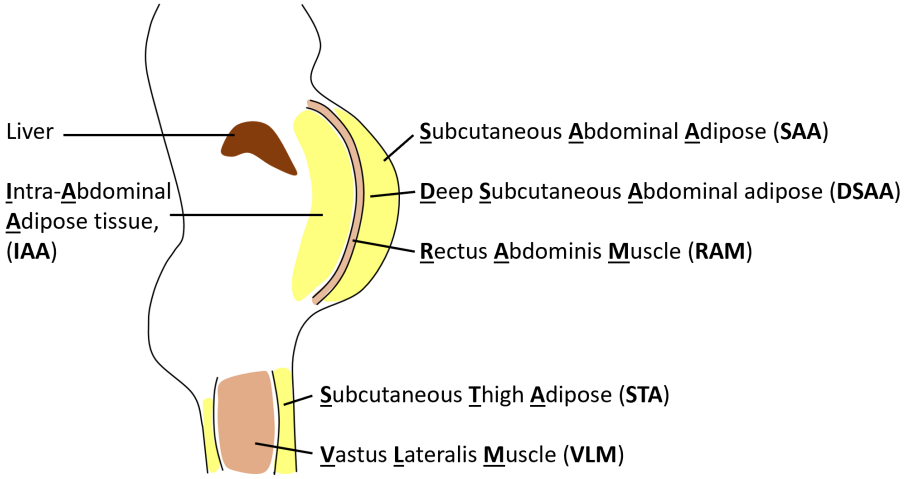

FIGURE 1 Schematic of the location of sites from which the seven tissue samples were collected for metabolomics analysis.

hoethanolamine (16:0 d_{31}-18:1-PE) was purchased from Avanti® (Avanti Polar Lipids, Alabaster, AL, USA). The extraction solvent of chloroform/methanol (v/v, 50:50) containing 16 mg/L pre-dissolved internal standards (d_5-L-tryptophan, d_4-citric acid, d_{10}-leucine, d_2-tyrosine, d_{35}-stearic acid, d_5-benzoic acid, ^{13}C-glucose, d_7-alanine) was stored at −20°C. A modified Folch solution (chloroform/methanol/water, v/v/v, 66:33:1) containing 0.01% (%w/v) pre-dissolved 16:0 d_{31}-18:1-Phosphoethanolamine internal standard for reconstitution of organic extract was also stored at −20°C freezer. Acetonitrile/water (v/v, 50:50) for reconstitution of the polar extract was stored at 4°C.

2.3 | Metabolomics analysis

Metabolite extraction was performed with 100 μl plasma or 25 mg frozen tissue using a bi-phasic extraction method previously described.[24] Briefly, tissue was homogenized in 800 μl prechilled extraction solvent with a single bead per tube for 2 × 60 s at 30 Hz, followed by addition of 400 μl water, vortex-mixing (2 × 15 s) and centrifugation (11 000 rpm, 4°C, 10 min). The plasma samples were mixed with 800 μl prechilled extraction solvent, agitated for 30 s and placed in a −20°C freezer for 60 min to allow protein precipitation, followed by addition of 400 μl water, vortex-mixing (2 × 15 s) and centrifugation (11 000 rpm, 4°C, 10 min). Finally, 200 μl of the upper aqueous layer and 200 μl of the bottom organic layer were transferred into two separate 2 ml microcentrifuge tubes separately, evaporated under a stream of nitrogen and stored at −80°C until analysis. All remaining upper phase or lower phase from the same sample type were combined to construct an aqueous or organic pool respectively for each sample matrix, aliquoted into 200 μl and evaporated under a stream of nitrogen for quality control (QC) sample construction. Blank samples were prepared following the same protocol but without the presence of tissue or plasma samples.

On the day of analysis, dried extracts were reconstituted in an appropriate volume of reconstitution solvent and analyzed as previously described. Briefly, dried polar extracts were reconstituted in 800 μl reconstitution solvent, separated on a SeQuant® ZIC®-pHILIC 5 μm, 2.1 mm × 100 mm column (Merck, Germany) and analyzed by a Thermo LC–MS system consisting of an Accela 1250 quaternary UHPLC pump coupled to an Exactive Orbitrap mass spectrometer (Thermo Fisher Scientific, Waltham, MA, USA). Samples were analyzed in both positive electrospray ionization (ESI+) and negative electrospray ionization (ESI−). Dried organic extracts (lipidome) reconstituted in 200 μl (plasma), 400 μl (liver), 800 μl (muscle), and 2000 μl (AT) reconstitution solvent were separated on an Acquity CSH™ C18 column 1.7 μm, 2.1 mm × 100 mm (Waters, USA) and analyzed by a Thermo LC–MS system comprising an Accela 1250 quaternary UHPLC system coupled to a Q Exactive hybrid quadrupole-Orbitrap mass spectrometer (Thermo Fisher Scientific, Waltham, MA, USA) using both ESI+ and ESI− modes.

Raw datafiles were converted to mzXML format with the ProteoWizard tool MSconvert (v 3.0.1818[25]) and pre-processed with XCMS (v3.0.2) altogether in R (v3.2.2)[26] so that the feature names could be aligned across the different sample types. The mega data matrix was then divided into subsets based on sample type and normalized by the same sample type pooled QC in the W4M Galaxy environment.[27] Blank features (defined as [nQC = 0], or [nQC ≠ 0, nBlank ≠ 0, tstat < 1 and $p < .05$ of QC over Blank generated by XCMS diffreport function]) and non-reproducible features (% coefficient of variation <30% in QC) were filtered out. Lipids were annotated using LipidSearch software v4.1.16 on representative MS^2 datafiles (Thermo Fisher Scientific, USA). Polar metabolites were annotated using an in-house library based on authentic standards (AgResearch) analyzed through HILIC LC–MS analysis under conditions identical to the current study. Unidentified features were searched against online databases including HMDB (http://www.hmdb.ca/), Metlin (http://metlin.scripps.edu/), and Lipid Maps (http://www.lipidmaps.org/) based on *m/z* with less than 10 ppm (for lipid features) or 15 ppm (for polar metabolite features) mass error.

2.4 | Statistical analyses

To justify the inclusion of samples and analysis of the GI surgery group ($n = 5$) with the bariatric surgery group ($n = 21$), principal component analysis (PCA) was carried out (Figure S1). One DSAA sample from the GI group was identified as a strong outlier for both the polar metabolites and lipids profile (Figure S2), hence was excluded from the subsequent analysis.

For each ESI mode of each analytical platform (polar and lipid), data analyses were performed in the following four steps:

1. A data matrix of paired plasma–tissue profiles containing annotated features common to both plasma and the tissue matrix (i.e., non-blank, reproducibly measured features) were constructed. Several participants did not have all tissue sites collected and participants with a plasma sample collected but no tissue sampled were excluded from analysis for that specific plasma–tissue matrix. A total number of 22 (STA), 22 (IAA), 19 (SAA), 25 (DSAA), 20 (VLM), 19 (RAM), and 24 (liver) datapoints were available for each plasma–tissue data matrix.

2. All profiles were normalized by BMI to eliminate its potentially confounding effect on metabolomic profiles, log-transformed and mean centered (auto-scaled) based on sample type. Pearson correlation analysis was applied on every paired feature in each plasma–tissue comparison.
3. To account for false positive discoveries (due to multiple comparison or processing artefacts), the p-value from the Pearson correlations were subjected to Benjamini–Hochberg multiple testing correction (BH corrected) for each paired plasma–tissue data matrix. A BH-corrected p-value <0.05 was considered statistically significant. Extracted ion chromatograms (EICs) from significantly correlated features were visually examined to further remove poorly integrated or misaligned features.
4. Any redundant features representing the same putative metabolite or lipid were also removed to report only individual lipid species/metabolites.

For polar metabolites showing significant correlation between plasma and tissues, enrichment analysis based on the Small Molecule Pathway Database (SMPDB) was performed on MetaboAnalyst (www.metaboanalyst.ca)[28] to understand metabolic pathways and network linked to these metabolites.

3 | RESULTS

3.1 | Lipidomic profiling and identification of significantly correlated lipids between plasma and seven tissue types

Results for ESI+ lipidomic analysis are summarized in Figure 2. A total number of 843 (ESI+) lipid features were annotated. Among the annotated lipid features analyzed by ESI+ mode, 553 (Plasma), 414 (STA), 449 (SAA), 447 (DSAA), 455 (IAA), 388 (VLM), 332 (RAM) and 482 (liver) features were detected in each tissue matrix (Table S2). Of these measured features, 265 (STA), 285 (SAA), 289 (DSAA), 261 (IAA), 307 (VLM), 280 (RAM), and 377 (liver) features were common between plasma and each corresponding tissue. For each plasma–tissue pair, 2 (STA), 4 (SAA), 24 (DSAA), 16 (IAA), and 202 (liver) features showed significant positive correlation between the plasma level and the tissue counterpart level (BH-corrected $p < .05$). No muscle lipid species measured by the ESI+ mode was correlated with plasma (Figure 2A). Plasma showed positive correlations with all four AT depots for various triglycerides (TG) species; the individual set of TGs correlated with each AT depot differed. A few other lipid species in plasma were also correlated with the abdominal subcutaneous adipose depots, including an ether-linked phosphatidylcholine (PC) species with SAA and a diglyceride (DG), a ceramide, a PC, and an ether-linked PC species with DSAA. Plasma lipid species correlated with the liver counterparts encompassed cholesterol esters (CEs), DG, TG, PC, phosphatidylethanolamines (PE), ether-linked PC, ether-linked PE, ceramide, and SMs (Figure 2B).

A total number of 472 (ESI−) lipid features were annotated (Figure 3A). Three hundred and fifty-five (Plasma), 83 (STA), 70 (SAA), 64 (DSAA), 80 (IAA), 158 (VLM), 150 (RAM), and 382 (liver) features were detected in each tissue matrix (Table S3). Of these, 76 (STA), 66 (SAA), 61 (DSAA), 73 (IAA), 137 (VLM), 133 (RAM), and 279 (liver) features were common to plasma and each corresponding tissue. For each plasma–tissue pair, 4 (STA), 2 (SAA), 4 (IAA), 10 (VLM), 12 (RAM), and 143 (liver) features showed significant positive correlation between the plasma level and the tissue counterpart level (BH-corrected $p < .05$). No DSAA lipid species measured by the ESI− mode were correlated with plasma. Plasma lipids showed positive correlations with three subtypes of AT and both subtypes of muscle for a range of phospholipids, while two ceramide species and one FFA in plasma were also correlated with SAT and VLM, respectively. Plasma lipid species encompassing ceramides, SM, mono- and dihexosylceramides, PC, PE, ether-linked PC, ether-linked PE, lysophosphatidylethanolamine (LPE), dimethyl-PE (PE-NMe2), and bilirubin were positively correlated with levels in the liver (Figure 3B).

By merging the significantly correlated lipid features identified by ESI+ and ESI− analyses together, plasma compared to liver provided the largest number of correlated lipid species (215 putative lipid species), followed by the deep central adipose depots (DSAA and IAA, 24 and 20, respectively) and subsequently the two subtypes of muscle tissue (RAM and VLM, 12 and 10 respectively). Plasma lipids were poorly correlated with their respective lipids in the superficial subcutaneous adipose depots including STA and SAA (<10 lipid species). Individual correlated lipid species and the statistical descriptions are provided in the Table S4.

Saturated and monounsaturated TGs in plasma were exclusively correlated with their levels in the liver. TGs of a lower degree of saturation (two to five double bonds) were correlated with their levels in liver and subcutaneous abdominal AT including both SAA and DSAA. Polyunsaturated TGs containing larger numbers of carbons (C ≥54, double bond ≥6) were correlated predominantly with their levels in the liver and the deep central AT depots including both the DSAA and IAA; two polyunsaturated TGs were also correlated with STA

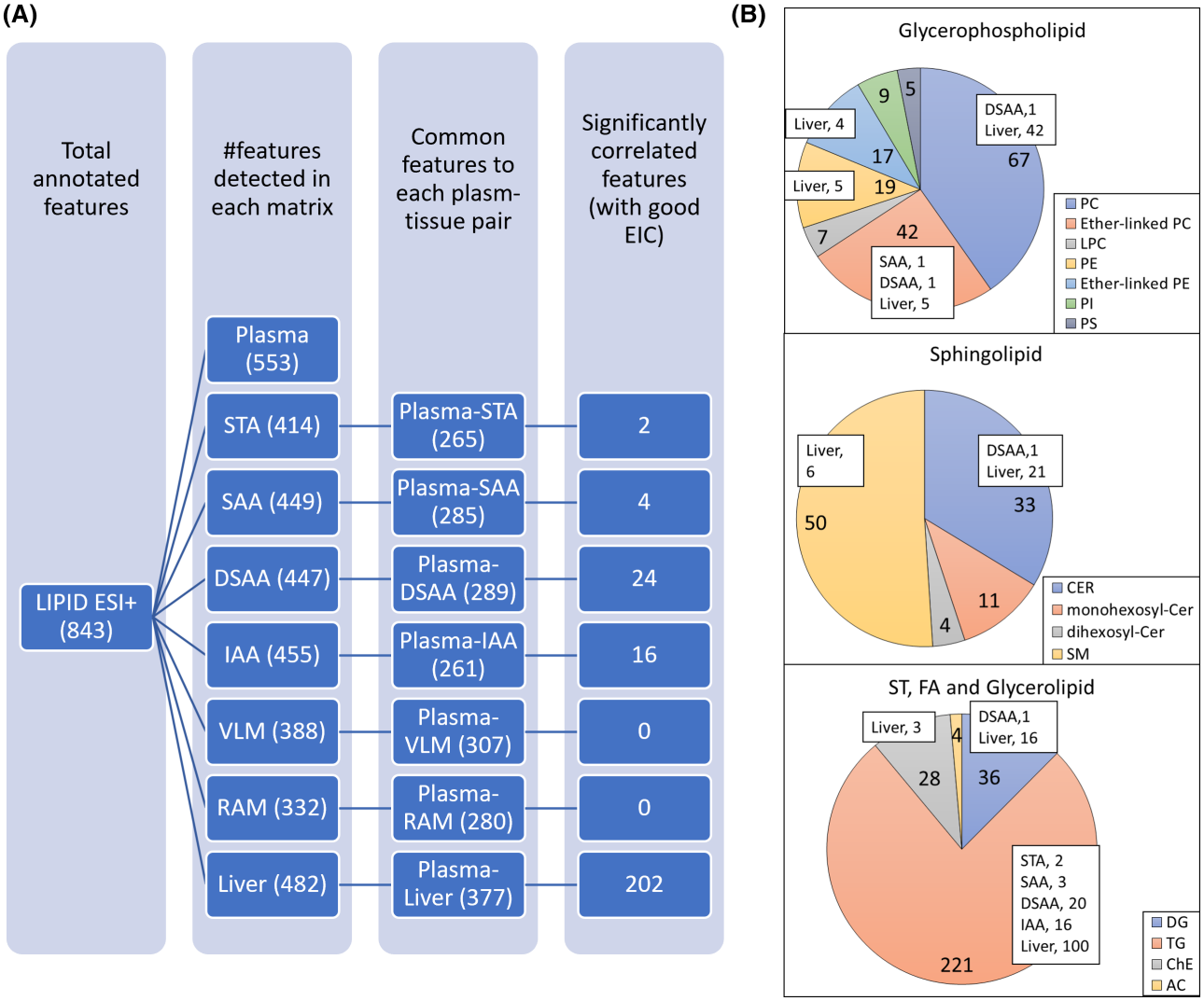

FIGURE 2 Characterization of lipid features measured by ESI+. (A) Number of features in each sample type and correlated features between plasma and each tissue type. (B) Number of annotated features in plasma (pie chart) and correlated features with their counterparts in different tissues (box). DSAA, deep subcutaneous abdominal adipose tissue; IAA, intra-abdominal adipose tissue; RAM, rectus abdominis muscle; SAA, subcutaneous abdominal adipose tissue; STA, subcutaneous thigh adipose tissue; VLM, vastus lateralis muscle.

(Figure 4). Overall, the plasma TG pool showed the greatest number of species correlated with the liver followed by the deep central AT depots (DSAA and IAA); only a small number were correlated with the superficial AT depots regardless of their locations in the upper or lower body (SAA and STA), and none were correlated with either muscle tissue at all. Among the 74 plasma TGs species correlated with liver, the top 3 most correlated TGs were all saturated species (TG 48:0, $r = 0.88$; TG 53:0, $r = 0.87$; TG 46:0, $r = 0.85$).

Several plasma sphingolipids encompassing subclasses of (dihydro)sphingomyelins, (dihydro)ceramides, deoxy-(dihydro)ceramides, were correlated with their levels in the liver. Ceramides containing 36–43 carbons and double bonds ≤1 were highly correlated between plasma and the liver ($r = 0.6$–0.84), whereas those containing very long chain (C = 44) and/or two double bonds were moderately correlated ($r = 0.45$–0.6). Likewise, the most highly correlated SMs between plasma and the liver were those containing 36–43 carbons and double bonds ≤1 ($r = 0.5$–0.84); while the least correlated (yet still significantly) SMs were those containing shorter chain (carbon <36) and/or two double bonds ($r = 0.45$–0.5) (Table S4). Two plasma ceramides also correlated with STA ceramides (Cer(d40:1), Cer(m42:2)).

Plasma FFA showed positive correlations with the liver for FFA (18:0) and FFA (20:5), and with VLM for FFA (18:1) (Table S4). No correlation was observed between plasma and AT FFA levels. Plasma phospholipids (PC, PE, ether-linked PC and ether-linked PE) showed positive correlations with all seven tissue types, however, the individual species differed (Table S4).

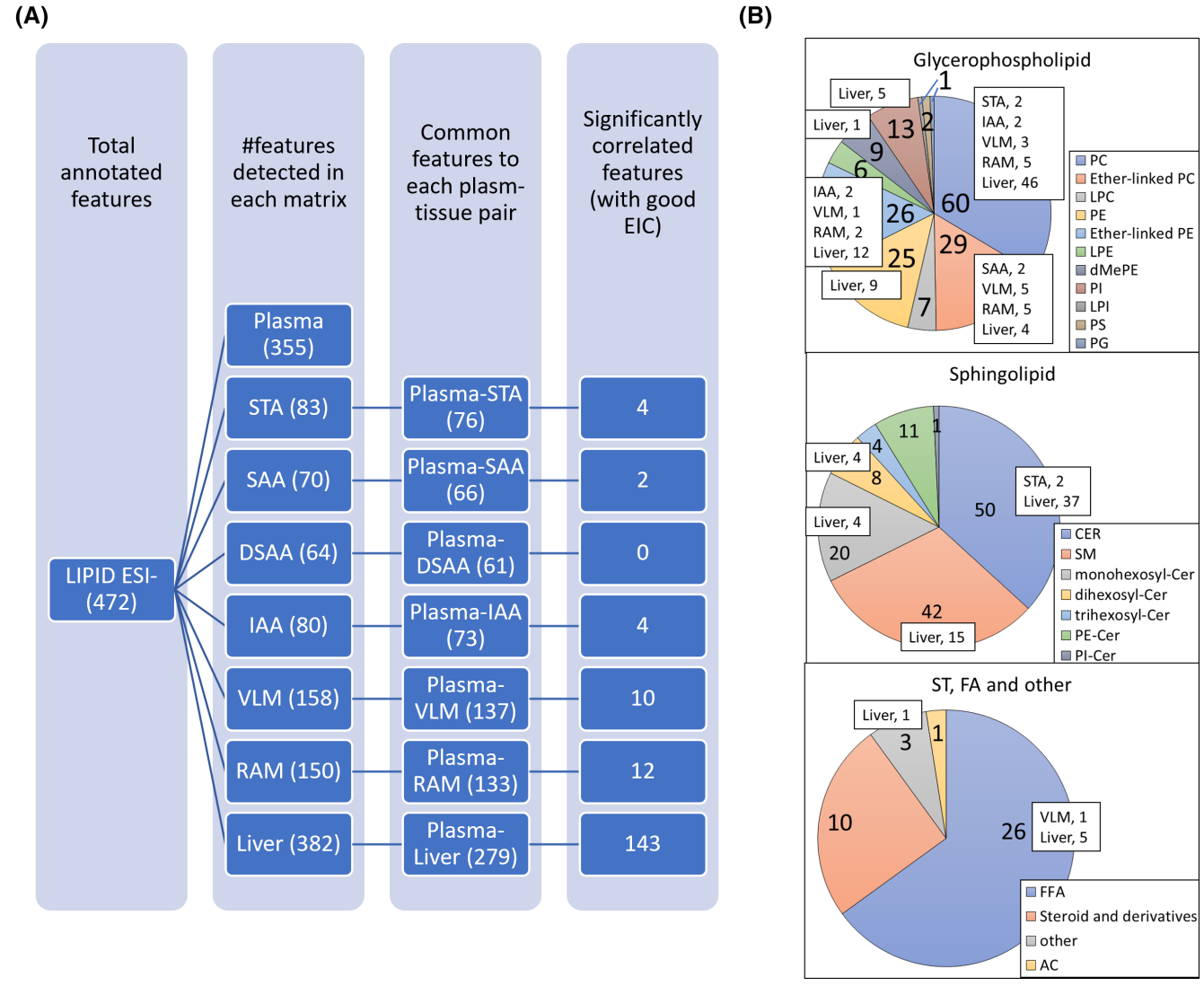

FIGURE 3 Characterization of lipid features measured by ESI−. (A) Number of features in each sample type and correlated features between plasma and each tissue type. (B) Number of annotated features in plasma (pie chart) and correlated features with their counterparts in different tissues (box). DSAA, deep subcutaneous abdominal adipose tissue; IAA, intra-abdominal adipose tissue; RAM, rectus abdominis muscle; SAA, subcutaneous abdominal adipose tissue; STA, subcutaneous thigh adipose tissue; VLM, vastus lateralis muscle.

Bilirubin and several lipid species belonging to CE, mono- and di-hexosylceramides, LPE and PE-NMe2 in plasma were only correlated with the corresponding species in the liver.

3.2 | Metabolomic profiling and identification of significantly correlated polar metabolites between plasma and seven tissue types

Results for the polar metabolite (HILIC) data are summarized in Figure 5. A total number of 162 (ESI+) polar metabolite features were annotated. Of these, 73 (Plasma), 59 (STA), 42 (SAA), 41 (DSAA), 62 (IAA), 108 (VLM), 94 (RAM), and 119 (liver) features were detected in each tissue matrix (Table S5). Among features common to plasma and each corresponding tissue, 3 (STA), 1 (SAA), 3 (IAA), 16 (VLM), 15 (RAM), and 27 (liver) features showed significant correlation between its plasma level and the tissue counterpart (BH-corrected $p < .05$). For ESI− analysis of polar metabolites, 31 features were annotated (Table S6), and plasma metabolites only displayed positive correlations for 1 (STA), 3 (VLM), and 1 (liver) features.

By collating the significantly correlated polar metabolite features identified by ESI+ and ESI− analyses together, the greatest number of plasma metabolites were correlated with its liver counterpart (28 features accounting for 28 putative metabolites), followed by the two subtypes of muscle tissue (between 10 and 20 metabolites); plasma polar metabolites were poorly correlated

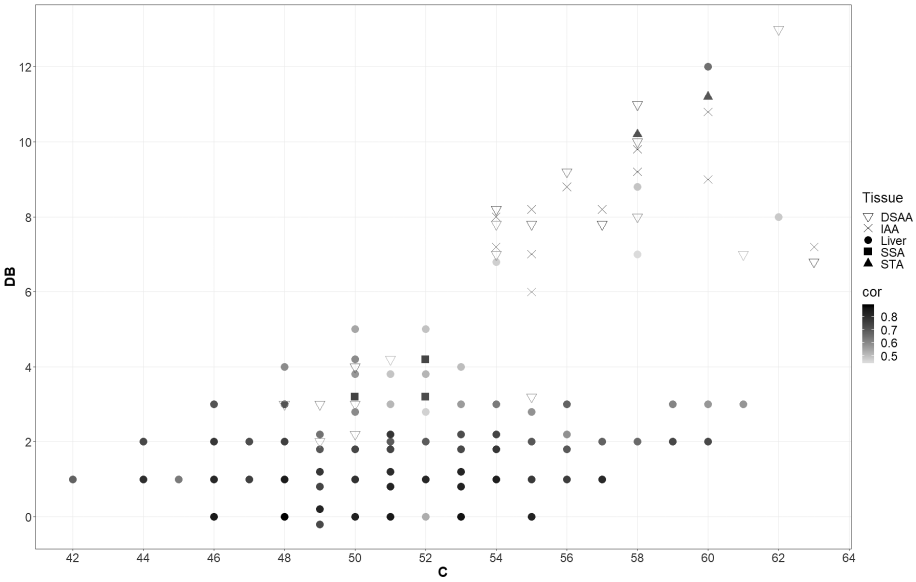

FIGURE 4 Composition of TG species in plasma showing significant correlations (BH $p < .05$) with the corresponding species in the liver or AT depots. C, total number of carbons; DB, total number of double bonds; DSAA, deep subcutaneous abdominal adipose tissue; IAA, intra-abdominal adipose tissue; SAA, subcutaneous abdominal adipose tissue; STA, subcutaneous thigh adipose tissue.

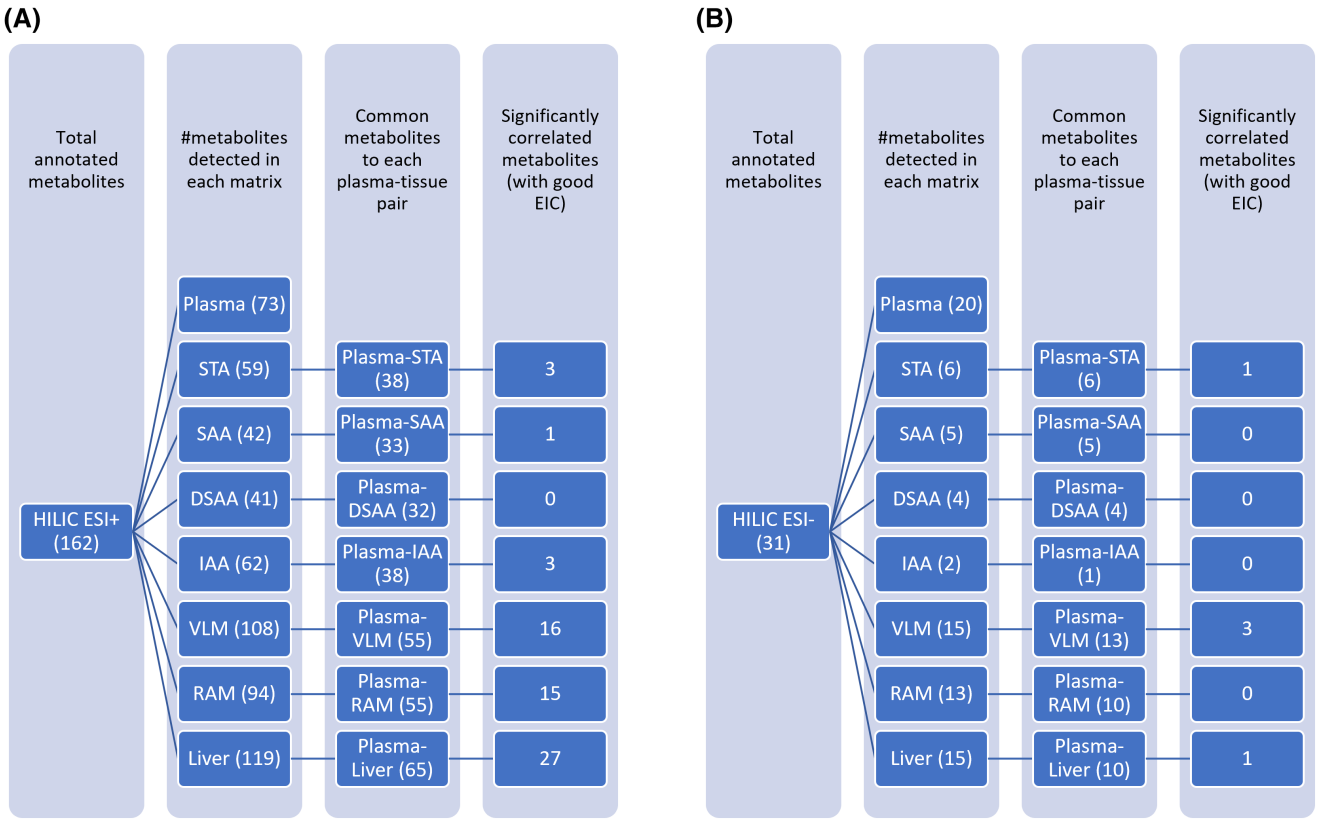

FIGURE 5 Number of polar metabolite (HILIC) features in each sample type and correlated features between plasma and each tissue type measured by ESI+ (A) and ESI− (B). DSAA, deep subcutaneous abdominal adipose tissue; IAA, intra-abdominal adipose tissue; RAM, rectus abdominis muscle; SAA, subcutaneous abdominal adipose tissue; STA, subcutaneous thigh adipose tissue; VLM, vastus lateralis muscle.

with their levels in AT regardless of the site of the depots (<10 metabolites). Individual correlated metabolites and the statistical descriptions are provided in Table S7.

Positive correlations were identified between plasma and muscle tissues mainly for metabolites linked with amino acid (AA) metabolism (Figure 6). Plasma also

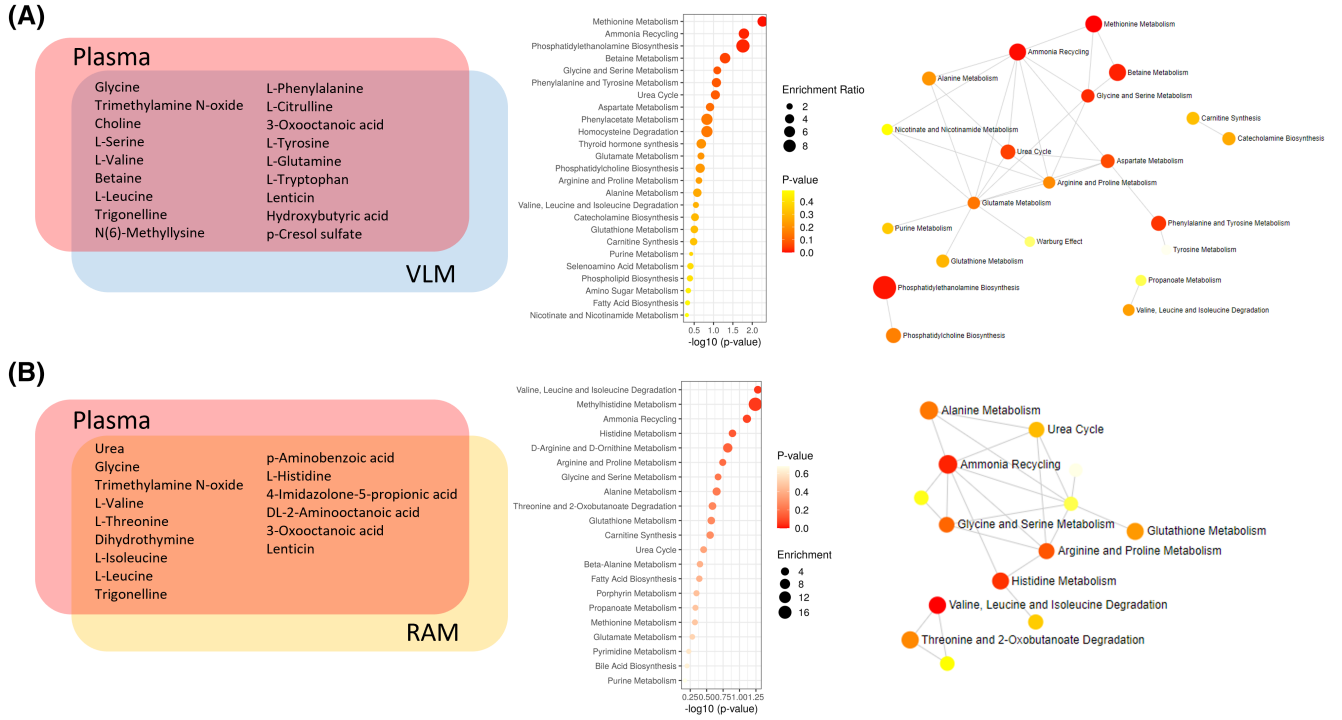

FIGURE 6 Individual polar metabolites showing significant correlation between plasma and muscle tissues of (A) VLM, and (B) RAM (BH $p < .05$), and the metabolic pathways linked to these metabolites analyzed by pathway enrichment and network analysis based on the Small Molecule Pathway Database (SMPDB). RAM, rectus abdominis muscle; VLM, vastus lateralis muscle.

showed significantly positive correlations with liver for metabolites linked with AA metabolism, energy metabolism, and fatty acid metabolism (Figure 7).

4 | DISCUSSION

Metabolomics has become widely applied to characterize plasma profiles associated with diseases and to identify metabolite markers. However, understanding the biological relevance of a plasma candidate marker can be challenging if it is unknown which site of tissue abnormality it reflects. The primary goal of the present study is to understand the relationship of metabolomic profile between plasma and various tissue types including AT, muscle, and liver, and to identify the set of plasma metabolites that can be used as a proxy for their tissue counterparts. Without prior knowledge or assumptions, our study found that the plasma lipidome is more reflective of the liver than other tissue types examined. Two hundred and two lipid features accounting for 151 putative lipid species measured by ESI+, and 143 lipid features accounting for 115 lipid species measured by ESI− showed significant positive correlations between plasma and liver. These lipid species collectively encompassed the lipid classes of ceramide, mono- and di-hexosylceramide, SM, PC, PE, LPE, PE-NMe2, ether-linked PC, ether-linked PE, FFA, CE, DG, and TG. Conversely, only a modest number of plasma lipids showed positive correlations with muscle or ATs. The set of lipid species correlated with muscle consisted of polar lipids whereas those correlated with ATs mainly comprised the highly hydrophobic TGs.

Likewise, the greatest number of plasma polar metabolites measured by the HILIC LC–MS platform were found to be correlated with concentrations in the liver. This included numerous AAs (e.g., valine, threonine, tryptophan), metabolites linked with energy metabolism (e.g., creatinine, carnitine), FA metabolism (e.g. 3-oxooctanoic acid, hydroxybutyric acid), cysteine and homocysteine metabolism (e.g., betaine, methionine), and gut microbial metabolites (e.g., trimethylamine oxide (TMAO), p-aminobenzoic acid, and ergothioneine). A modest number of plasma polar metabolites were also found to be correlated with concentrations in muscle tissues, including a range of AAs and related metabolites, gut microbial metabolites and xenobiotics that were mainly involved in AA metabolism. In contrast, plasma polar metabolites were poorly correlated with AT depots, likely owing to the less aqueous cellular environment of AT.

Further to the primary goal, the present study also sought to identify, if any, inter-depot or regional differences in the metabolomic relationship between plasma and AT or muscle. Despite being at different locations, both RAM and VLM showed positive correlations with plasma for

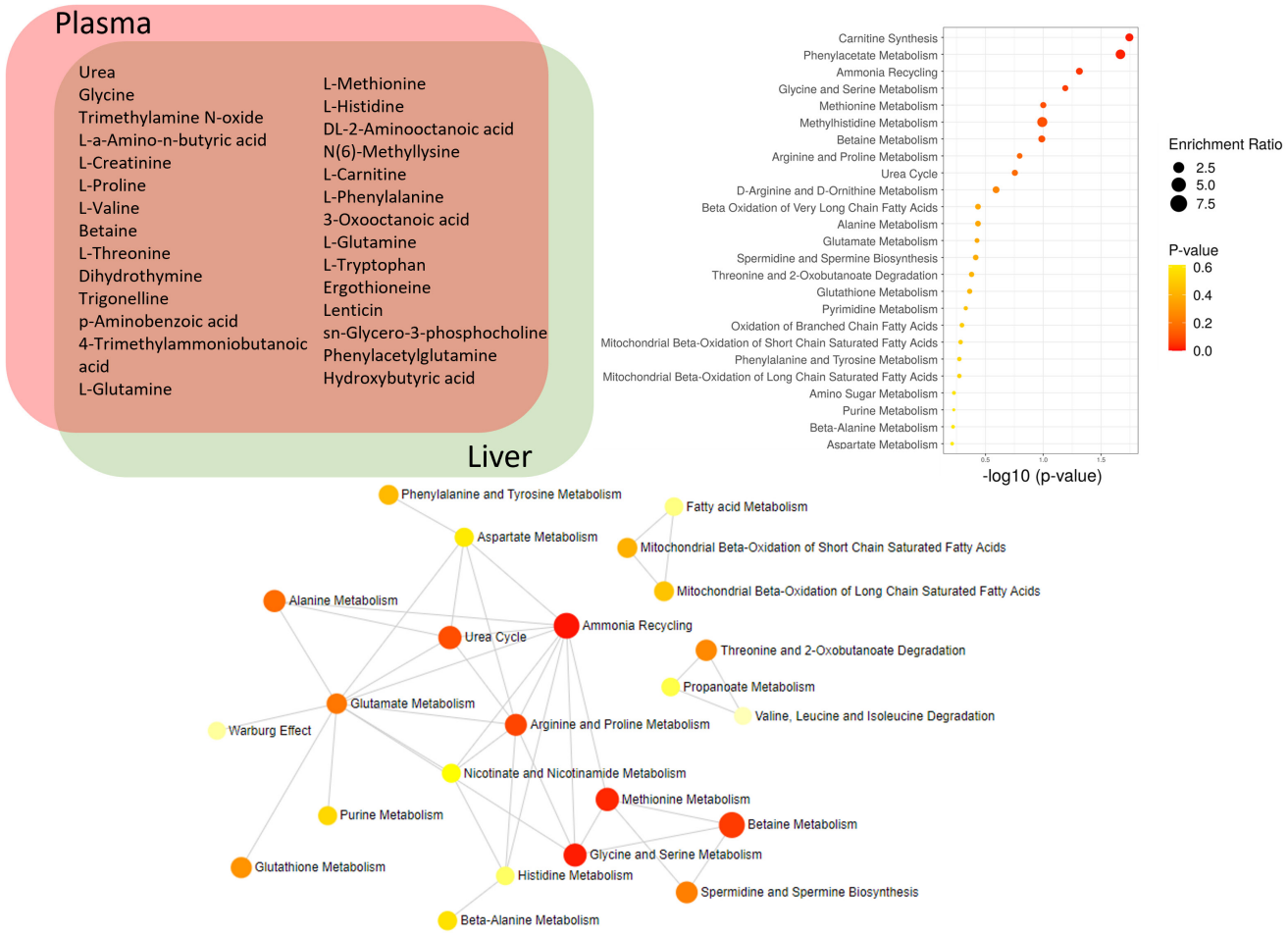

FIGURE 7 Individual polar metabolites showing significant correlation between plasma and the liver (BH $p < .05$), and the metabolic pathways linked to these metabolites analyzed by pathway enrichment and network analysis based on the Small Molecule Pathway Database (SMPDB).

several long-chain polyunsaturated fatty acid (LCPUFA)-containing PC, ether-linked PC, ether-linked PE, AAs and related metabolites, and gut microbial metabolites. This is likely owing to the fact that they both belong to skeletal muscle and were collected after an overnight fast. On the other hand, it is well established that the intra-abdominal AT compartment is biologically distinct from subcutaneous AT as they exhibit different expression profiles, metabolic activity, and pro-inflammatory potential.[29] Based on substantive evidence of epidemiological associations, regional distribution of body fat is differentially associated with cardiometabolic risk.[30] When dissecting the role and contribution of individual adipose depots to cardiometabolic risks, the intra-abdominal adipose and thigh adipose depots were found to be detrimental and protective, respectively,[23,31] whereas the role of abdominal subcutaneous depots, which can be further divided into superficial or deep AT, remains controversial.[32–35] Four adipose depots located at three different sites (lower body subcutaneous: STA, upper body subcutaneous: SAA and DSAA, and intra-abdominal: IAA) were investigated in the present study. Overall, all four depots showed some similarities in their metabolomic relationships with plasma: (1) poor correlations were observed for the vast majority of polar metabolites; only a few non-endogenous metabolites such as xenobiotics and gut microbial metabolites were correlated; (2) positive correlations were observed for a number of PUFA-containing TGs. There was no clear discrimination regarding their metabolomic relationships with plasma between different compartments (intra-abdominal vs. subcutaneous) or depots associated with different types of regional obesity (central vs. peripheral). Instead, the number of correlated TGs notably decreased as the location of adipose depot shifted from the deeper abdominal site (i.e., IAA, DSAA) toward superficial abdominal or peripheral sites (i.e., SAA, STA). This finding suggested regional differences of AT contributing to the plasma TG pool, and that the plasma TG profile is slightly more reflective of the TG profile of the deep central, risky adipose depots than the peripheral, safe adipose depots.

To the best of our knowledge, this is the first study to comprehensively measure and correlate metabolites in

human plasma and several tissues. Two LC-MS platforms were adopted and both ionization modes were carried out to increase metabolome coverage. Major limitations of the present study included a small sample size and that two groups with different baselines were pooled together for analysis. To justify the inclusion of samples from the GI group for analysis, PCA was carried out to confirm the similarity of the metabolomic profile between the two groups as well as to identify outliers. Another limitation is that this cross-sectional study only provided a single-timepoint snapshot of the relationship between plasma and various tissues, based on the relative quantification across samples, and thus did not imply dynamics or direction of metabolic flux. Without healthy lean control, it is impossible to confirm whether the lipid derangement pattern in the plasma lipidome is a consequence of abnormal lipid metabolism of the liver or due to the breakdown of adipose tissue. Additionally, the inability of the present method to measure a wide range of exogenous metabolites makes it difficult to draw conclusions relating to diet or gut microbiota. Nonetheless, findings from the present study could rationalize or consolidate the use of several candidate metabolite markers for clinical diagnosis and risk screening.

Plasma bilirubin can reflect liver function, metabolism, and excretion of bile and has been an important component to calculate a prognostic score for liver disease.[36] A model comprising plasma bilirubin and creatinine (along with the prothrombin time) to predict mortality at the end stage of liver disease was developed.[37] Our results showed direct linear relationships between liver and plasma concentrations of bilirubin and creatinine, despite the participants were of normal range of ALT and AST. This finding provided further confirmation to support the validity and robustness of these metabolites as more sensitive biomarkers for diagnosis and prognosis of liver disease.

Previous lipidomics studies have highlighted differential cardiometabolic risks associated with different sets of plasma TG species. TG species containing a lower total carbon number and fewer unsaturated bonds were prominently associated with fatty liver diseases, incident cardiovascular disease and increased risk of T2D, whereas those containing high carbon number and greater degree of unsaturation were associated with a decreased risk of T2D.[38–41] In the present study, levels of saturated and monounsaturated TGs in plasma were exclusively correlated with their levels in the liver, while PUFA-containing TGs were correlated with their levels in ATs. Interestingly, a recent study has shown that plasma levels of several saturated and monounsaturated TGs are predictive of excessive liver fat at early stage, whereas increased VAT/SAT ratio can be reflected by several PUFA-containing TGs.[42] Complementary to biomarker discovery studies, our results indicated that the set of plasma TGs identified as potential predictors for poor cardiometabolic health are likely reflective of an abnormal level in the liver, possibly attributable to a higher rate of de novo lipogenesis, TG synthesis and very low-density lipoprotein secretion. On the contrary, TG species potentially acting as negative predictors for cardiometabolic risk, may reflect their storage in AT depots likely indicating protection against cardiometabolic diseases.

Disruption of lipid balance involved in sphingolipid metabolism has been frequently associated with T2D,[43–49] and postulated to be linked with inflammation, insulin resistance (IR), and oxidative stress.[43,49,50] Several lines of evidence have demonstrated a role of ceramide as a lipid mediator that exerts a range of cellular effects.[51] Yet a deeper understanding and interpretation remains challenging without knowing whether the changes of a range of related metabolites resulting from perturbed sphingolipids metabolism are confined within local tissue sites or can be readily detectable in the circulation. Herein, we reported that a majority of plasma sphingolipids, on a broad scale, including ceramide, SMs, and glycosphingomyelins, showed strong correlations with their counterparts in the liver. The correlated SMs and ceramides between plasma and liver showed chain length-specificity, mainly for those containing a very long acyl chain fatty acids (VLCFAs) such as C22:0, C24:0, and C24:1, in line with a previous finding that CerS2, a ceramide synthase showing substrate specificity for longer acyl chain species, was predominantly expressed in the liver.[52,53] Our results provided evidence supporting the liver to be a major source of plasma VLCFA-containing ceramides and SMs. Given the concentrations were well correlated, changes in this subset of sphingolipids in plasma may capture an abnormal handling and metabolism of sphingolipids in the liver.

DG has also been long recognized as a mediator of IR in the liver and muscle via the suppression of the insulin signaling pathway,[54–56] and increased circulating DG was reported in cases of prediabetes and T2D.[48] Herein, we observed positive correlations of DG between plasma and the liver, suggesting abnormally high levels of circulating DG reported in dysglycemia may reflect increased level in the liver and thus be indicative of the development of liver IR.

Plasma FFA composition has been hypothesized to be an indicator of AT FFA composition since AT lipolysis is a major source of plasma FFA. However, findings from existing studies have been inconsistent.[13,14] In the present study, we did not observe any correlations between plasma and FFA levels in the various types of AT. Instead, plasma FFAs were found to be correlated with FFA contents in the liver (FA 18:0, 20:5) and VL muscle (FA 18:1).

Positive correlations for several plasma PC species with multiple tissues were observed. PCs are a major

component of cellular membranes and therefore are ubiquitous throughout the body. Interesting patterns for the correlated PC species were noticed. A broad scale of tissues (STA, DSAA, IAA, VLM, RAM, and liver) exhibited positive correlations with plasma for PUFA-containing PC species. Plasma PC species that contained a lower even total carbon number (C≤34) and a monounsaturated fatty acid chain were correlated with the more central tissue sites (IAA, RAM, and liver). Saturated PC species as well as odd chain-containing PC species in plasma were exclusively correlated with their liver counterparts. Our results suggested differential contributions from various tissues to the plasma PC pool.

Accumulating evidence from recent metabolomics studies have shown an inverse association between plasma ether-linked phospholipids and cardiometabolic diseases.[48,57–59] Ether-linked phospholipids are peroxisome-derived moieties and play a structural role as membrane components.[60] They may also act as signaling molecules and have antioxidant properties.[60] However, the source and implication of plasma ether-linked phospholipids are less well understood. Our results revealed that several plasma ether-linked PC species reflected levels in the liver, both subcutaneous depots (DSAA and SAA) and both muscle tissues, while plasma ether-linked PE species reflected levels in the liver, IAA, and both muscle tissues.

Plasma AAs were found to be positively correlated with concentrations in the muscles and liver. This is as expected since protein turnover in the muscle and liver is increased during fasting and thus likely to act as a major contributor to the plasma AA pool at the time of sampling.[61–63]

Dysregulation of cysteine and homocysteine metabolism has been implicated in the development of fatty liver diseases,[64] and this pathway plays a critical role in maintaining liver health.[65,66] Unsurprisingly, concentrations of several metabolites linked to this pathway such as methyl donor replenishers (e.g., betaine and methionine), and methylated products (e.g., N(6)-methyllysine and trigonelline) also showed positive correlations between plasma and liver.

Trimethylamine (TMA) is produced by gut microbiota and the liver is the site of first pass metabolism that oxidizes TMA to TMAO.[67] Therefore, liver is the primary source for circulating TMAO, and a strong correlation between its concentration in the liver and plasma is observed as expected. Interestingly, TMAO was also positively correlated with concentrations in the muscle. A TMAO transporter has been recently identified and characterized; therefore its accumulation in tissues is possible.[68] Concentrations of several other microbial metabolites in plasma (e.g., p-aminobenzoic acid, p-cresol sulfate, and ergothioneine) were also found to be correlated with ATs, muscles, and/or the liver. Although the metabolism, distribution, and biological implication of these microbial metabolites are less well characterized, our findings provided evidence for their accumulation in biological tissues. In light of the current view that gut microbiota impact metabolic health, whether these metabolites play a biological role and mediate the effects of gut microbiota on host health could warrant future research.

5 | CONCLUSION

In conclusion, the plasma lipidomic profile from obese but otherwise healthy, premenopausal human females is mostly reflective of the liver profile, while several plasma phospholipid species and TG species were also correlated with concentrations in the muscle and AT, respectively. Regional differences were observed for the correlation between plasma TGs and their counterparts in various adipose depots, with the plasma TG profile being more reflective of the deep abdominal adipose depots that are generally considered as risky than the superficial abdominal or peripheral adipose depots that may be less detrimental or even protective. The plasma polar metabolite profile is more reflective of the liver and muscle for metabolites mainly linked to amino acid and energy metabolism, but poorly correlated with AT profile. Our study confirms that the overall plasma metabolomic profile provides a window for monitoring metabolites in multiple tissue types, and various constituents of the plasma metabolomic profile can be used as a proxy for tissue metabolites. Given that the plasma metabolomics profile is more reflective of some tissues (e.g. the liver) but not others (e.g. ATs), our study also highlighted the critical importance of taking into consideration the correlation between plasma metabolites and tissue counterparts when linking a plasma metabolite marker to an underlying mechanisms occurring in a specific tissue. Incorrect attribution of plasma markers to less relevant tissue sites may lead to erroneous assumption and mechanism speculations.

AUTHOR CONTRIBUTIONS

Anne-Thea McGill and Ivana R. Sequeira were involved in conceptualization, clinical design and management, sample collection, and storage and handling. Zhanxuan E. Wu was involved in methodology, sample preparation and extraction, metabolomics data acquisition, data analysis, data visualization and presentation, and writing—original draft. Marlena Kruger, Sally D. Poppitt, Garth J. S. Cooper, and Karl Fraser were involved in writing—review and editing. Marlena Kruger, Sally D. Poppitt, and Karl Fraser were involved in supervision. Sally D. Poppitt and Garth J. S. Cooper were involved in funding acquisition.

ACKNOWLEDGMENTS

This study was funded by the New Zealand Ministry for Business, Innovation and Employment (MBIE, grant no. 3710040) through the High Value Nutrition National Science Challenge and New Zealand Health Research Council (HRC, grant no.08/190C). We thank Dr. Heike Schwendel (AgResearch) for technical assistance and guidance with the LC–MS instrumental analysis.

DISCLOSURES

The authors declare no conflict of interest.

DATA AVAILABILITY STATEMENT

The original data are available from the corresponding author upon request.

ORCID

Zhanxuan E. Wu https://orcid.org/0000-0003-1896-0221

REFERENCES

1. Newgard CB. Metabolomics and metabolic diseases: where do we stand? *Cell Metab*. 2017;25(1):43-56.
2. Gika H, Theodoridis G. Sample preparation prior to the LC–MS-based metabolomics/metabonomics of blood-derived samples. *Bioanalysis*. 2011;3(14):1647-1661.
3. Psychogios N, Hau DD, Peng J, et al. The human serum metabolome. *PLoS One*. 2011;6(2):e16957.
4. Quehenberger O, Armando AM, Brown AH, et al. Lipidomics reveals a remarkable diversity of lipids in human plasma. *J Lipid Res*. 2010;51(11):3299-3305.
5. McGranaghan P, Saxena A, Rubens M, et al. Predictive value of metabolomic biomarkers for cardiovascular disease risk: a systematic review and meta-analysis. *Biomarkers*. 2020;25(2):101-111.
6. Carter TC, Rein D, Padberg I, et al. Validation of a metabolite panel for early diagnosis of type 2 diabetes. *Metabolism*. 2016;65(9):1399-1408.
7. Gao X, Ke C, Liu H, et al. Large-scale metabolomic analysis reveals potential biomarkers for early stage coronary atherosclerosis. *Sci Rep*. 2017;7(1):1-11.
8. Hong X, Zhang B, Liang L, et al. Postpartum plasma metabolomic profile among women with preeclampsia and preterm delivery: implications for long-term health. *BMC Med*. 2020;18(1):1-12.
9. Johnson CH, Ivanisevic J, Siuzdak G. Metabolomics: beyond biomarkers and towards mechanisms. *Nat Rev Mol Cell Biol*. 2016;17(7):451-459.
10. Naz S, Moreira dos Santos DC, García A, Barbas C. Analytical protocols based on LC–MS, GC–MS and CE–MS for non-targeted metabolomics of biological tissues. *Bioanalysis*. 2014;6(12):1657-1677.
11. Jové M, Moreno-Navarrete JM, Pamplona R, Ricart W, Portero-Otín M, Fernández-Real JM. Human omental and subcutaneous adipose tissue exhibit specific lipidomic signatures. *FASEB J*. 2014;28(3):1071-1081.
12. Kotronen A, Seppänen-Laakso T, Westerbacka J, et al. Comparison of lipid and fatty acid composition of the liver, subcutaneous and intra-abdominal adipose tissue, and serum. *Obesity*. 2010;18(5):937-944.
13. Hellmuth C, Demmelmair H, Schmitt I, Peissner W, Blüher M, Koletzko B. Association between plasma nonesterified fatty acids species and adipose tissue fatty acid composition. *PLoS One*. 2013;8(10):e74927.
14. Walker CG, Browning LM, Stecher L, et al. Fatty acid profile of plasma NEFA does not reflect adipose tissue fatty acid profile. *Br J Nutr*. 2015;114(5):756-762.
15. Soeters M, Sauerwein H, Duran M, et al. Muscle acylcarnitines during short-term fasting in lean healthy men. *Clin Sci*. 2009;116(7):585-592.
16. Bélanger C, Hould F-S, Lebel S, Biron S, Brochu G, Tchernof A. Omental and subcutaneous adipose tissue steroid levels in obese men. *Steroids*. 2006;71(8):674-682.
17. Rangel-Huerta OD, Pastor-Villaescusa B, Gil A. Are we close to defining a metabolomic signature of human obesity? A systematic review of metabolomics studies. *Metabolomics*. 2019;15(6):1-31.
18. Guasch-Ferré M, Hruby A, Toledo E, et al. Metabolomics in prediabetes and diabetes: a systematic review and meta-analysis. *Diabetes Care*. 2016;39(5):833-846.
19. Ruiz-Canela M, Hruby A, Clish CB, Liang L, Martínez-González MA, Hu FB. Comprehensive metabolomic profiling and incident cardiovascular disease: a systematic review. *J Am Heart Assoc*. 2017;6(10):e005705.
20. Gruzdeva O, Borodkina D, Uchasova E, Dyleva Y, Barbarash O. Localization of fat depots and cardiovascular risk. *Lipids Health Dis*. 2018;17(1):1-9.
21. Al-Sari N, Suvitaival T, Mattila I, et al. Lipidomics of human adipose tissue reveals diversity between body areas. *PLoS One*. 2020;15(6):e0228521.
22. Schleinitz D, Krause K, Wohland T, et al. Identification of distinct transcriptome signatures of human adipose tissue from fifteen depots. *Eur J Hum Genet*. 2020;28(12):1714-1725.
23. Tchkonia T, Thomou T, Zhu YI, et al. Mechanisms and metabolic implications of regional differences among fat depots. *Cell Metab*. 2013;17(5):644-656.
24. Wu ZE, Kruger MC, Cooper GJ, Poppitt SD, Fraser K. Tissue-specific sample dilution: an important parameter to optimise prior to untargeted LC-MS metabolomics. *Metabolites*. 2019;9(7):124.
25. Chambers MC, Maclean B, Burke R, et al. A cross-platform toolkit for mass spectrometry and proteomics. *Nat Biotechnol*. 2012;30(10):918-920.
26. Smith CA, Want EJ, O'Maille G, Abagyan R, Siuzdak G. XCMS: processing mass spectrometry data for metabolite profiling using nonlinear peak alignment, matching, and identification. *Anal Chem*. 2006;78(3):779-787.
27. Van Der Kloet FM, Bobeldijk I, Verheij ER, Jellema RH. Analytical error reduction using single point calibration for accurate and precise metabolomic phenotyping. *J Proteome Res*. 2009;8(11):5132-5141.
28. Pang Z, Chong J, Zhou G, et al. MetaboAnalyst 5.0: narrowing the gap between raw spectra and functional insights. *Nucleic Acids Res*. 2021;49(W1):W388-W396.
29. Lafontan M, Berlan M. Do regional differences in adipocyte biology provide new pathophysiological insights? *Trends Pharmacol Sci*. 2003;24(6):276-283.

30. Vega GL, Adams-Huet B, Peshock R, Willett D, Shah B, Grundy SM. Influence of body fat content and distribution on variation in metabolic risk. *J Clin Endocrinol Metab*. 2006;91(11):4459-4466.
31. Snijder MB, Visser M, Dekker JM, et al. Low subcutaneous thigh fat is a risk factor for unfavourable glucose and lipid levels, independently of high abdominal fat. The Health ABC Study. *Diabetologia*. 2005;48(2):301-308.
32. Walker GE, Verti B, Marzullo P, et al. Deep subcutaneous adipose tissue: a distinct abdominal adipose depot. *Obesity*. 2007;15(8):1933-1943.
33. Kim S-H, Chung J-H, Song S-W, Jung WS, Lee Y-A, Kim H-N. Relationship between deep subcutaneous abdominal adipose tissue and metabolic syndrome: a case control study. *Diabetol Metab Syndr*. 2016;8(1):1-9.
34. Sam S. Differential effect of subcutaneous abdominal and visceral adipose tissue on cardiometabolic risk. *Horm Mol Biol Clin Investig*. 2018;33(1):20180014.
35. Elffers TW, de Mutsert R, Lamb HJ, et al. Body fat distribution, in particular visceral fat, is associated with cardiometabolic risk factors in obese women. *PLoS One*. 2017;12(9):e0185403.
36. Méndez-Sánchez N, Vítek L, Uribe M. *Bilirubin as a biomarker in liver disease*. Springer; 2017:281-304.
37. Kamath PS, Wiesner RH, Malinchoc M, et al. A model to predict survival in patients with end-stage liver disease. *Hepatology*. 2001;33(2):464-470.
38. Mayo R, Crespo J, Martínez-Arranz I, et al. Metabolomic-based noninvasive serum test to diagnose nonalcoholic steatohepatitis: results from discovery and validation cohorts. *Hepatol Commun*. 2018;2(7):807-820.
39. Orešič M, Hyötyläinen T, Kotronen A, et al. Prediction of non-alcoholic fatty-liver disease and liver fat content by serum molecular lipids. *Diabetologia*. 2013;56(10):2266-2274.
40. Stegemann C, Pechlaner R, Willeit P, et al. Lipidomics profiling and risk of cardiovascular disease in the prospective population-based Bruneck study. *Circulation*. 2014;129(18):1821-1831.
41. Rhee EP, Cheng S, Larson MG, et al. Lipid profiling identifies a triacylglycerol signature of insulin resistance and improves diabetes prediction in humans. *J Clin Investig*. 2011;121(4):1402-1411.
42. Wu ZE, Fraser K, Kruger MC, et al. Untargeted metabolomics reveals plasma metabolites predictive of ectopic fat in pancreas and liver as assessed by magnetic resonance imaging: the TOFI_Asia study. *Int J Obes*. 2021;45(8):1844-1854.
43. Haus JM, Kashyap SR, Kasumov T, et al. Plasma ceramides are elevated in obese subjects with type 2 diabetes and correlate with the severity of insulin resistance. *Diabetes*. 2009;58(2):337-343.
44. Samad F, Hester KD, Yang G, Hannun YA, Bielawski J. Altered adipose and plasma sphingolipid metabolism in obesity: a potential mechanism for cardiovascular and metabolic risk. *Diabetes*. 2006;55(9):2579-2587.
45. de Mello VDF, Lankinen M, Schwab U, et al. Link between plasma ceramides, inflammation and insulin resistance: association with serum IL-6 concentration in patients with coronary heart disease. *Diabetologia*. 2009;52(12):2612-2615.
46. Yin X, Willinger CM, Keefe J, et al. Lipidomic profiling identifies signatures of metabolic risk. *EBioMedicine*. 2020;51:102520.
47. Wigger L, Cruciani-Guglielmacci C, Nicolas A, et al. Plasma dihydroceramides are diabetes susceptibility biomarker candidates in mice and humans. *Cell Rep*. 2017;18(9):2269-2279.
48. Meikle PJ, Wong G, Barlow CK, et al. Plasma lipid profiling shows similar associations with prediabetes and type 2 diabetes. *PLoS One*. 2013;8(9):e74341.
49. Xu F, Tavintharan S, Sum CF, Woon K, Lim SC, Ong CN. Metabolic signature shift in type 2 diabetes mellitus revealed by mass spectrometry-based metabolomics. *J Clin Endocrinol Metab*. 2013;98(6):E1060-E1065.
50. Sui J, He M, Wang Y, Zhao X, He Y, Shi B. Sphingolipid metabolism in type 2 diabetes and associated cardiovascular complications. *Exp Ther Med*. 2019;18(5):3603-3614.
51. Chaurasia B, Summers SA. Ceramides–lipotoxic inducers of metabolic disorders. *Trends Endocrinol Metab*. 2015;26(10):538-550.
52. Riebeling C, Allegood JC, Wang E, Merrill AH, Futerman AH. Two mammalian longevity assurance gene (LAG1) family members, trh1 and trh4, regulate dihydroceramide synthesis using different fatty acyl-CoA donors. *J Biol Chem*. 2003;278(44):43452-43459.
53. Laviad EL, Albee L, Pankova-Kholmyansky I, et al. Characterization of ceramide synthase 2 tissue distribution, substrate specificity, and inhibition by sphingosine 1-phosphate. *J Biol Chem*. 2008;283(9):5677-5684.
54. Itani SI, Ruderman NB, Schmieder F, Boden G. Lipid-induced insulin resistance in human muscle is associated with changes in diacylglycerol, protein kinase C, and IκB-α. *Diabetes*. 2002;51(7):2005-2011.
55. Samuel VT, Liu Z-X, Qu X, et al. Mechanism of hepatic insulin resistance in non-alcoholic fatty liver disease. *J Biol Chem*. 2004;279(31):32345-32353.
56. Erion DM, Shulman GI. Diacylglycerol-mediated insulin resistance. *Nat Med*. 2010;16(4):400-402.
57. Floegel A, Stefan N, Yu Z, et al. Identification of serum metabolites associated with risk of type 2 diabetes using a targeted metabolomic approach. *Diabetes*. 2013;62(2):639-648.
58. Graessler J, Schwudke D, Schwarz PE, Herzog R, Shevchenko A, Bornstein SR. Top-down lipidomics reveals ether lipid deficiency in blood plasma of hypertensive patients. *PLoS One*. 2009;4(7):e6261.
59. Bagheri M, Farzadfar F, Qi LU, et al. Obesity-related metabolomic profiles and discrimination of metabolically unhealthy obesity. *J Proteome Res*. 2018;17(4):1452-1462.
60. Dean JM, Lodhi IJ. Structural and functional roles of ether lipids. *Protein Cell*. 2018;9(2):196-206.
61. Li JB, Higgins JE, Jefferson LS. Changes in protein turnover in skeletal muscle in response to fasting. *Am J Physiol Endocrinol Metab*. 1979;236(3):E222-E228.
62. Ruderman NB. Muscle amino acid metabolism and gluconeogenesis. *Annu Rev Med*. 1975;26(1):245-258.
63. De Blaauw I, Deutz N, Von Meyenfeldt M. In vivo amino acid metabolism of gut and liver during short and prolonged starvation. *Am J Physiol Gastrointest Liver Physiol*. 1996;270(2):G298-G306.
64. Pacana T, Cazanave S, Verdianelli A, et al. Dysregulated hepatic methionine metabolism drives homocysteine elevation in diet-induced nonalcoholic fatty liver disease. *PLoS One*. 2015;10(8):e0136822.
65. Jung Y-S. Metabolism of sulfur-containing amino acids in the liver: a link between hepatic injury and recovery. *Biol Pharm Bull*. 2015;38(7):971-974.
66. Mato JM, Martinez-Chantar ML, Lu SC. Methionine metabolism and liver disease. *Annu Rev Nutr*. 2008;28:273-293.
67. Janeiro MH, Ramírez MJ, Milagro FI, Martínez JA, Solas M. Implication of trimethylamine N-oxide (TMAO) in disease: potential biomarker or new therapeutic target. *Nutrients*. 2018;10(10):1398.

68. Teft WA, Morse BL, Leake BF, et al. Identification and characterization of trimethylamine-N-oxide uptake and efflux transporters. *Mol Pharm*. 2017;14(1):310-318.

SUPPORTING INFORMATION

Additional supporting information may be found in the online version of the article at the publisher's website.

How to cite this article: Wu ZE, Kruger MC, Cooper GJS, et al. Dissecting the relationship between plasma and tissue metabolome in a cohort of women with obesity: Analysis of subcutaneous and visceral adipose, muscle, and liver. *FASEB J*. 2022;36:e22371. doi:10.1096/fj.202101812R